Prediction of premature separation of bonded CFRP plates from strengthened steel beams using a fracture criterion

A. Lenwari† and T. Thepchatri‡

Department of Civil Engineering, Chulalongkorn University, Bangkok 10330, Thailand

E. Watanabe‡

Department of Civil Engineering, Kyoto University, Kyoto 606-8501, Japan

Abstract. This paper presents a method for predicting premature separation of carbon fiber reinforced plastic (CFRP) plates from strengthened steel beams. The fracture criterion based on material-induced singularity is formulated in terms of a singular intensity factor. Static test on double strap joints was selected to provide the critical stress intensity factor in the criterion because good degree of accuracy and consistency of experimental data can be expected compared with the unsymmetrically loaded single lap joints. The debond/separation loads of steel beams with different CFRP lengths were measured and compared with those predicted from the criterion. Good agreement between the test results and the prediction was found.

Key words: fracture; stress singularity; strengthening; CFRP; steel beams; bridges; bi-material wedges; double strap joints.

1. Introduction

The application of bonded composite repair for rehabilitation/strengthening of steel bridge structures so far has been limited. Feasibility study by Sen *et al.* (1995) indicated the possibility of this method on strengthening steel-concrete composite beams. For bridge structures, fatigue is an important limit state. Steel beams with partial length welded cover plates are classified in the category having the lowest fatigue strength AASHTO (1996) and JSSC (1995). From this point, adhesive bonding is more appealing than welding. In addition, the use of lightweight composites is easy and minimally disrupts traffic. Therefore, the use of bonded composites for strengthening steel beams was investigated, including the design and analysis of bonded plates.

One possible failure mode in bonded composite repair is the premature separation of bonded plates from the steel beams. This failure mode is unfavorable and greatly reduces the effectiveness of the strengthening scheme.

---

† Ph.D. Student
‡ Professor

This paper presents a fracture criterion and the method for predicting the premature separation observed in the experiments on steel beams with different lengths of CFRP plates bonded to the bottom flanges. It was realized that there is a material-induced singularity at the plate end (cut-off point) and any stress (or strain) criterion may be unsuitable for predicting debond/separation of bonded plates from steel beams due to fracture occurring at the plate end.

2. Theory

2.1 Stress singularity at bimaterial wedges

When two materials with different elastic properties are joined forming a bimaterial wedge, stress singularity will be present at the apex of this bimaterial wedge under mechanical or thermal loading if linear elasticity is assumed. Fig. 1(a) shows a general bimaterial wedge and Fig. 1(b) shows the bimaterial wedge in this study. The stress field near the singular point is given by

$$\sigma_{ij}(r, \theta) = \sum_{k=1}^{N} \frac{K}{(r/L)^{\lambda_k}} \cdot f_{ijk}(\theta) + \sigma_{ijo}(\theta) \tag{1}$$

Where r and θ are the polar coordinates, N is the number of r-dependent stress terms, and L is a characteristic length of the configuration. It was shown by Bogy (1971) that λ_k are the solutions of a transcendental equation and are dependent on the elastic constants of the two materials and the angles θ_1 and θ_2. $f_{ijk}(\theta)$ is a function dependent on the angle θ. The regular term, $\sigma_{ijo}(\theta)$, and the generalized stress intensity factor, K, are dependent on the loading and global geometry.

For the case of $N = 1$, if point A in Fig. 1(b) is approached along the y-axis the normal stress in y-direction, for small y-values ($r/L \ll 1$), will be

$$\sigma_y = Q\left(\frac{r}{L}\right)^{-\lambda_1}, \quad (\lambda > 0) \tag{2}$$

Where Q and λ_1 are constants. Q was denoted as stress intensity factor in this study. Since the free edge is free from tractions, one can express the vertical displacements (u_y) in the vicinity of point A
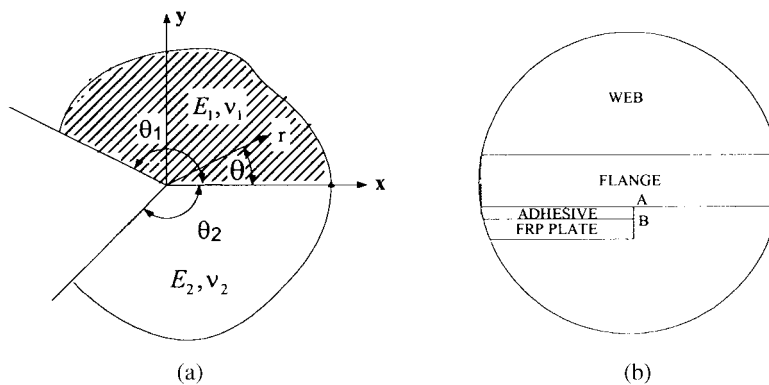

Fig. 1 (a) General bimaterial wedge, (b) singularity at the plate cut-off point A and B are singular points

in terms of λ_1 and Q simply by integrating the normal strain (ε_y). In this way one obtains

$$u_y = \frac{QL\xi^{1-\lambda_1}}{E^*(1-\lambda_1)} + u_{yo} \tag{3}$$

In Eq. (3), ξ is y non-dimensionalized with respect to L, E^* equals to $E/(1-v^2)$ and E for plane strain and plane stress, respectively, and u_{yo} is the regular vertical displacement of the point A. The stress intensity factor was, then, calculated from Eq. (3).

2.2 Fracture criterion

It is proposed that fracture will occur when:

$$Q = Q_{cr} \tag{4}$$

Where Q_{cr} is the critical stress intensity factor. This value was selected to be obtained from the tests on double-strap joints. Double strap joints were proposed since good degree of accuracy and consistency of test results can be expected compared with the unsymmetrically loaded single lap joints. The joints must have the following properties same as the strengthened steel beams: adhesive type, bimaterial wedge angles and steel surface preparation. The value of Q_{cr} obtained will then be used to predict the fracture load, P_{cr}, which leads to the separation of the bonded plate from the steel beam, by using the relation:

$$P_{cr} = \frac{Q_{cr}}{Q_{FEM}} P_{FEM} \tag{5}$$

Where P_{FEM} and Q_{FEM} are the applied load in the finite element model and the Q-factor calculated from the finite element analysis, respectively.

2.3 Calculation of stress intensity factor

The finite element model of double strap joints is shown in Fig. 2. Quarter of the joint was modeled because of symmetry. Fig. 3 shows the model of the strengthened beam in the analysis. Half of the beam was modeled due to symmetry. CFRP material was assumed isotropic. The elements used were 8-node elements having two degree of freedom at each node. The finite element program ANSYS was used. Table 1 shows the material properties used in the analysis. Some preliminary meshes showed that it was necessary to use a finer mesh near the singular point to evaluate proper values of stress singularity parameter. Submodeling technique was used in which the specified boundary conditions for the submodel were obtained from displacements calculated on the
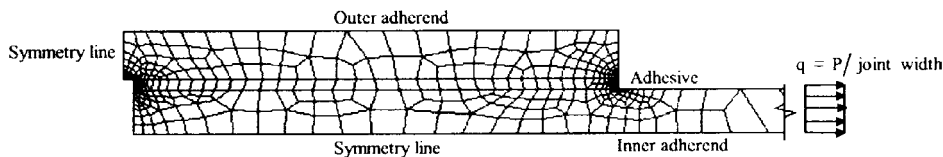

Fig. 2 Finite element mesh for a double-strap joint (Quarter model, see Fig. 5)
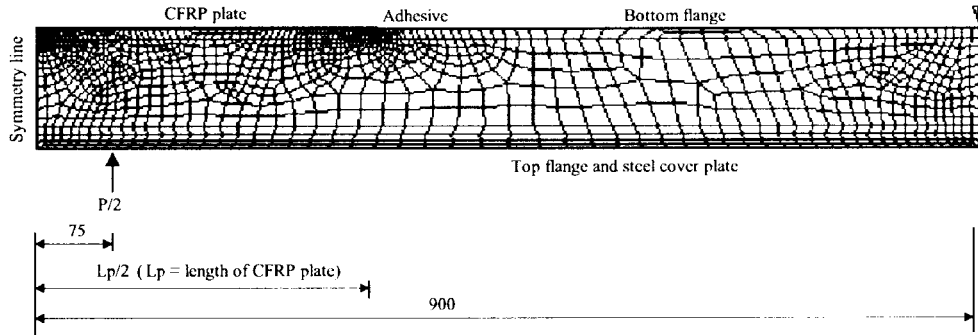
Fig. 3 Finite element mesh for a strengthened beam (Half model, see Fig. 8)

Table 1 Material data

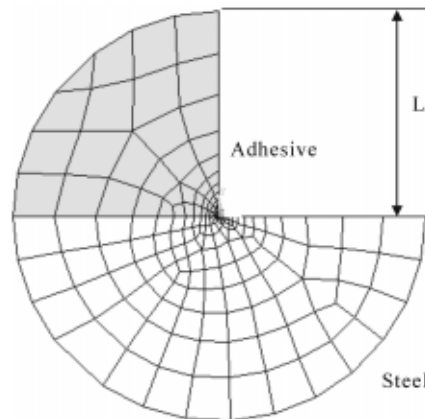| Steel: JIS SS400	Adhesive: SIKADUR-30	CFRP: SIKA H514
E = 200000 MPa	E = 2750 MPa	E = 300000 MPa
v = 0.30	v = 0.35	v = 0.30
Fy = 300 MPa	-	thickness = 1.4 mm.

Fig. 4 Submodel

cut boundary of the global model. Submodel for calculating stress intensity factor is shown in Fig. 4. The same submodel was used for both when double strap joints and the strengthened beams were the global model. The size of the smallest element near the singular point in the submodel was 0.00005 mm. By using Eq. (3) and taking L to be half of the adhesive layer thickness, the value of Q was determined as ξ approaches zero.

For the case of bimaterial wedge in this study (adhesive with E = 2750 MPa and v = 0.35 and steel with E = 200000 MPa and v = 0.3) and the wedge angles as shown in Fig. 1(b), it was found that λ_1 is 0.326. The assumption of plane strain was assumed since the steel was considered rigid compared with the adhesive and, further, the joint thickness was small compared with the joint width.

3. Experimental program

3.1 Static test on double strap joints

Double strap joint specimens are shown in Fig. 5. The joint was designed to prevent yielding of both inner and outer steel adherends. The average bond strength obtained from the preliminary test on similar joints was used for designing the lap length. The steel surface was sandblasted according to *The Steel Structure Painting Council Specification No.5* (1991). The thickness of adhesive layer was controlled by putting small inserts having diameter 1 mm between the adherends. The inserts were located away from the high stress region (e.g., from joint ends). Also, it is important that the terminus of the adhesive must be made sharp perpendicular to the steel surface according to Fig. 1(b) because the FE-model used this shape of terminus. All joints were tested at crosshead speed of 1.2 mm/min. The curing time was about 2 weeks.

Strain gages were attached to the joints to investigate the behaviors of the joints, e.g., the strain distribution and to verify the global finite element model. Fig. 6 compares the strain distribution
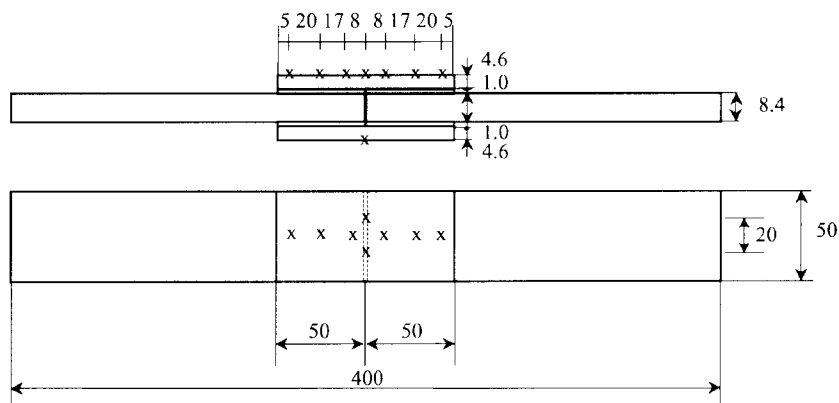

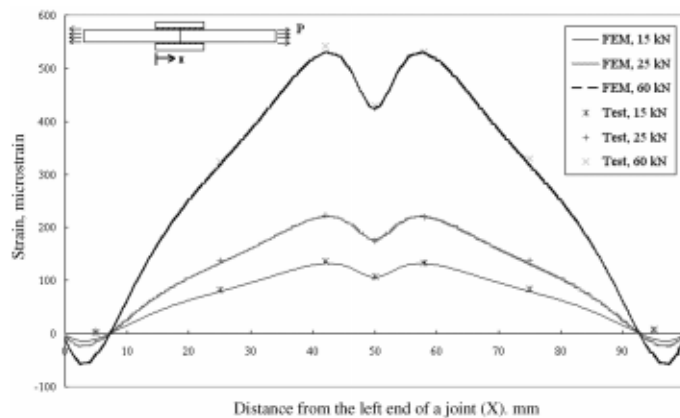Fig. 5 Double strap joints (All dimensions are in mm.)

Fig. 6 Strain distribution from FEM analysis v.s. measurement at various load levels
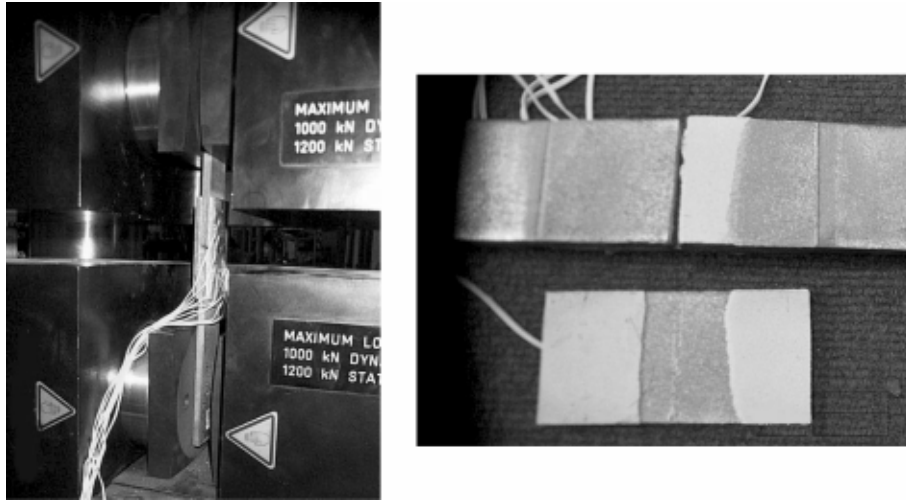
Fig. 7 (Left) Testing of double strap joints, (Right) typical failure of double strap joints

along outer adherends from 2-D finite element analysis with the test data at various load levels. Typical failure of the joints was adhesive failure between steel and adhesive as shown in Fig. 7.

3.2 Static test on strengthened steel beams

Test setup for steel beams strengthened with bonded CFRP plates is shown in Fig. 8. Three series with different CFRP lengths were investigated. Specimens were identified with a code that was composed of a letter and a number. The number referred to the length of CFRP plates in centimeter. For some specimens, yielding of steel flange at mid span had occurred, which simulated severe service distress, before attaching FRP plates. They were denoted having "Y" in specimen designation. Steel cover plates were welded to the top flanges of the W100 × 17.2 beams. The cover plate was designed to prevent compression yielding in the compression flange. All specimens were tested in four-point bending over a simple span. The loads were 150 mm apart. Strain gages were attached to both the FRP plates and the flanges of steel beams to verify the global finite element model and investigate the debond behavior.

Although spew fillet is the usual condition encountered in practice, the terminus of adhesive in the strengthened beams was made sharp perpendicular to steel surface corresponding to the terminus condition of double strap joints and finite element models.

4. Results and discussion

In the tests on double strap joints, the failure loads were measured. A critical value of stress intensity factor, Q_{cr}, in the fracture criterion was, then, calculated from the average fracture loads of all specimens tested. It was found that the average value with standard deviation of Q_{cr} was 39.59 ± 4.22 MPa (Lenwari and Thepchatri 2001).

Table 2 summarizes results from the tests on strengthened steel beams. The failure loads which

Table 2 Comparison between the prediction and the test results on steel beams with CFRP plates

Specimen	CFRP length (mm)	Failure mode[*]	(1) Failure load (kN)	(2) Prediction (kN)	RATIO=(1)/(2)
B50-1	500	Premature debond (L)	90.2	73.1	1.2
B50-2	500	Premature debond (L)	93.7	73.1	1.3
B65-1	650	Premature debond (L)	105.9	82.6	1.3
B65-2	650	Premature debond (R)	98.5	82.6	1.2
B65Y-1	650	Premature debond (R)	106.8	82.6	1.3
B120-1	1200	FRP rupture	143.0	159.5[**]	-
B120Y-1	1200	FRP rupture	155.2	159.5[**]	-

[*](L) denotes left end debond. (R) denotes right end debond.
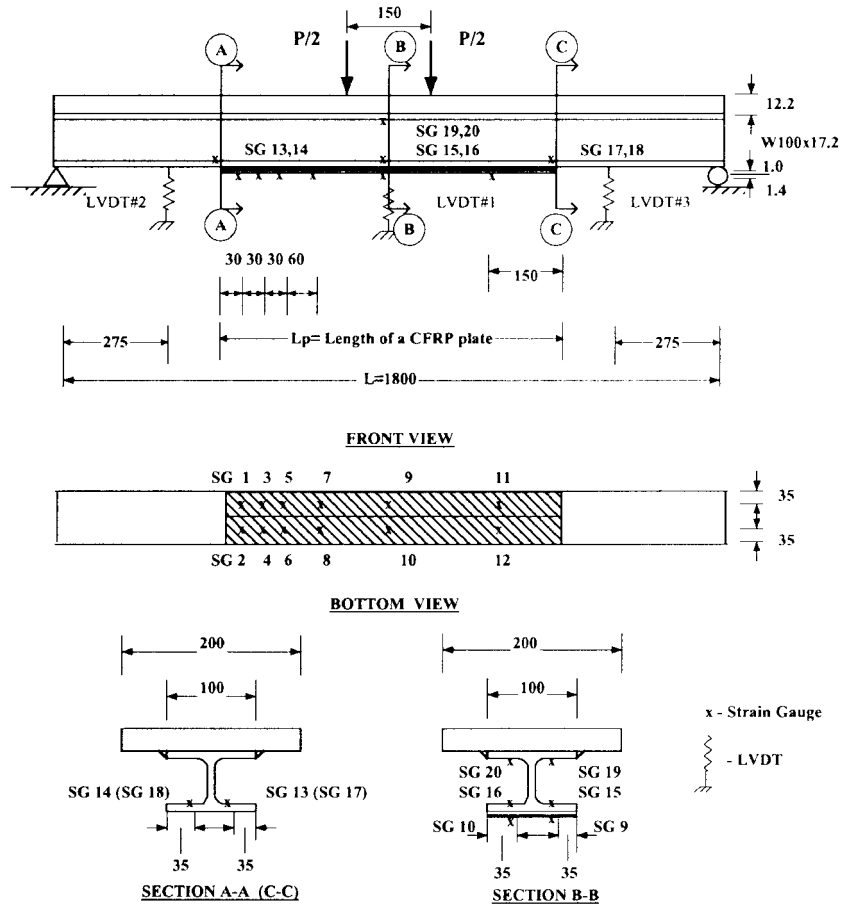[**]For FRP rupture mode, the prediction was made for debond failure mode.

Fig. 8 Test setup for the strengthened beams

led to complete separation of CFRP plates or rupture of CFRP plates are shown in the table. There was a premature separation in series B50 and B65. For series B120, rupture of CFRP plates at

Fig. 9 FRP rupture mode (B120-1)

Fig. 10 Premature separation mode (B65-1)

Table 3 Debond detection from strain gages SG13, 14 or SG17, 18 attached to the flange of a steel beam at the cut-off point (Criteria is the deviation from the elastic trend)

Specimen	Debond load, kN	Average load, kN	SD, kN
B50-1	65.2	70.3	7.2
B50-2	75.3		
B65-1	82.6		
B65-2	79.0	81.4	2.1
B65Y-1	82.6		

midspan occurred. Typical failure characteristics were shown in Figs. 9 and 10. For the premature separation mode, failure loads were measured from LVDT no.1 where the deflection increased dramatically. These values are very closed to those observed during the test.

It was found that, however, the initiation of debond/separation of FRP plates from steel beams had occurred before the final fracture which led to complete separation. These loads were detected by considering the increase in the strain value from the strain gage number 13 and 14 which were attached to steel flange at the plate cut-off points (in the case when left-end debond occurred) and strain gage number 17 and 18 (in the case when right-end debond occurred). The deviation of the strain from linear elastic trend indicated that the initiation of debond had occurred. This was because the stresses transferred to FRP plates decreased as the debond cracks propagated. The debond initiation occurred at the loads lower than the final debond loads where the debond cracks had propagated to the critical size. Finally, rapid crack propagation occurred due to fracture accompanied with a loud noise. Debond loads in Table 3 are loads when strains start having the percent differences from the linear elastic trendline exceeding the maximum percent difference of data scattering used in constructing the linear lines. A typical deviation from linear elastic trend is shown in Fig. 11.

It was found that the predicted loads agreed well with those leading to debond initiation from the tests. The differences between the prediction and the tests were 4% and 1.5% for series B50 and B65, respectively. Moreover, from Table 2, the ratio of final debond loads to the predicted loads was about 1.25. This indicates that the prediction underestimates the final debond loads which lead to
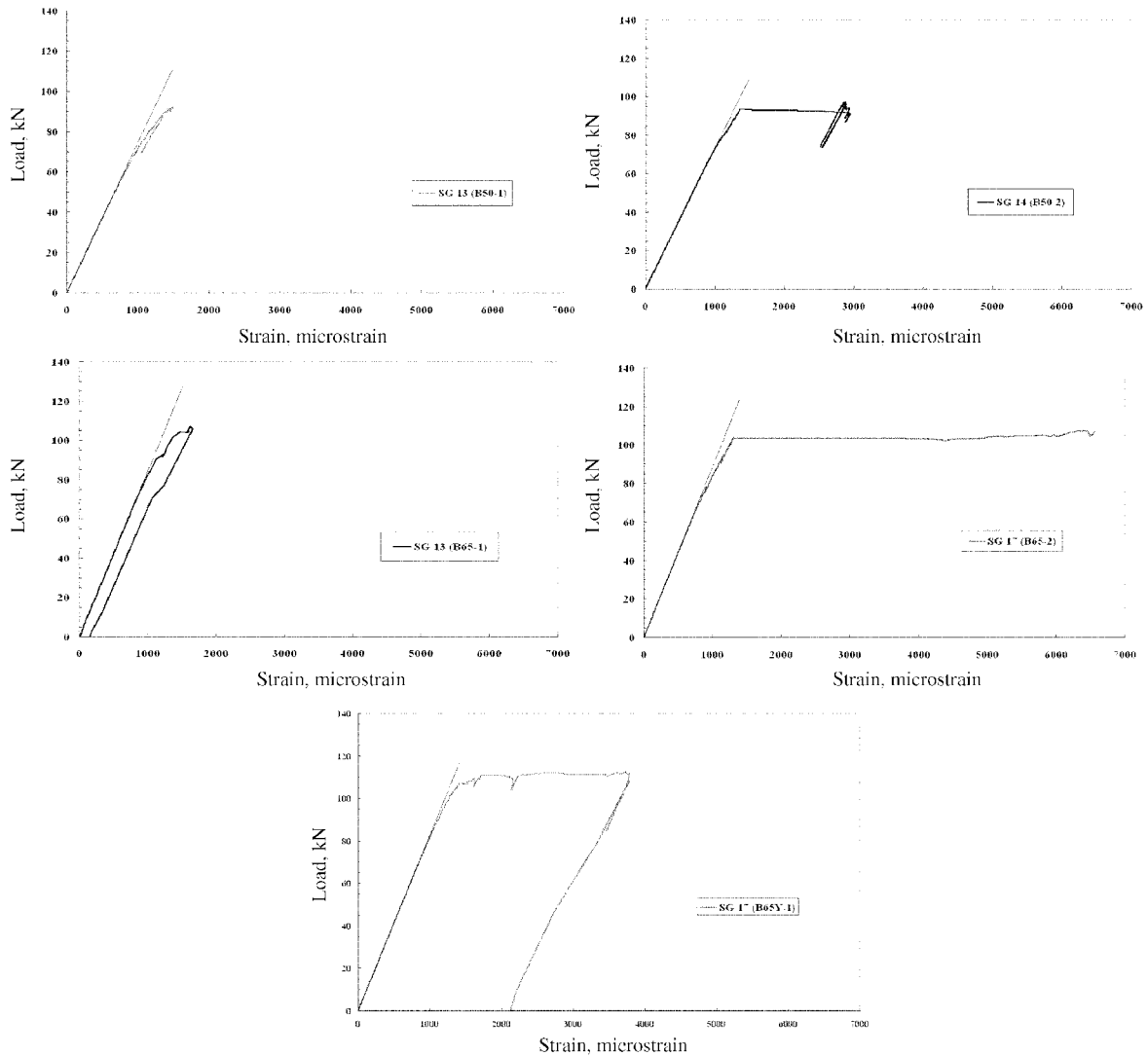
Fig. 11 Load-strain relationship for series B50 and B65 (for detecting debond initiation)

complete separation of CFRP plates from steel beams.

For B120-1 and B120Y-1, where the failure mode was FRP rupture at midspan, it can be seen that there was no deviation observed from strain gage number 13,14 (and strain gage number 17,18). For strain gage number 13 and 14, the relationship between load and measured strain is shown in Fig. 12.

5. Conclusions

Linear elastic fracture mechanics was found to be applicable to the debond problem in steel beams strengthened by bonded CFRP plates. This failure mode should be realized before the bonded composite repair can be applied to steel bridges such as steel-concrete composite bridges.
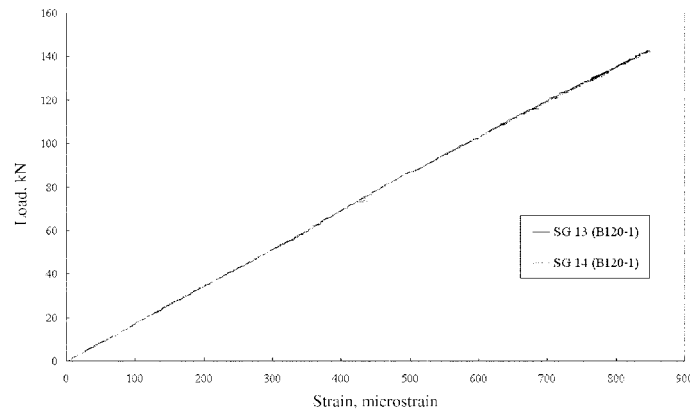
Fig. 12 Load-strain relationship (B120-1)

The cut-off points are usually located away from high stress region, so no general yielding occurs at the cut-off points. It was found that the fracture criterion using the critical stress intensity factor from static test on double-strap joints can be used to predict the debond initiation observed in the experiment on strengthened beams very well. The adhesive/steel interface (near the singular point A in Fig. 1(b)) is the most critical location for debond initiation. The surface preparation, adhesive type, and curing time of adhesive of the joints were controlled to be the same as the strengthened beams. This criterion may be useful with regard to linear elastic (brittle) adhesives.

Acknowledgements

References

American Association of State Highway Bridges, AASHTO (1996), *Standard Specifications for Highway Bridges*, 16th edition.

Bogy, D.B. (1971), "Two edge-bonded elastic wedges of different materials and wedge angles under surface tractions", *Transactions ASME, J. Appl. Mech.*, **38**, 377-386.

Groth, H.L. (1987), *Analysis of Adhesive Joints*, Report No. 87-17, Department of Aeronautical Structures and Materials, The Royal Institute of Technology, SWEDEN.

Japanese Society of Steel Construction, JSSC (1995), *Fatigue Design Recommendations for Steel Structures.*

Lenwari, A. and Thepchatri, T. (2001), "Prediction of failure load in steel beams bonded with CFRP plates due to fracture at plate ends using stress singularity parameter", *Proceedings of the fourteenth KKNN symposium on Civil Engineering, Kyoto, Japan,* 259-265.

Sen, R., Liby, L., Spillett, K. and Mullins, G. (1995), "Strengthening steel composite bridge members using CFRP laminates", *Non-metallic (FRP) Reinforcement for Concrete Structures, RILEM,* 551-558.

Steel Structures Painting Council (1991), *Surface Preparation*, Extracted from Vol. 2, *Systems and Specification*, 6th Edition, Pittsburgh, PA.